

Airplanes at constant speeds on inclined circular trajectories

Gilles Labonté*

Department of Mathematics and Computer Science and Department of Electrical Engineering and Computer Engineering, Royal Military College of Canada, Kingston, Ontario, Canada

(Received November 3, 2015, Revised December 12, 2015, Accepted December 27, 2015)

Abstract. The dynamical requirements are obtained for airplanes to travel on inclined circular trajectories. Formulas are provided for determining the load factor, the bank angle, the lift coefficient and the thrust or power required for the motion. The dynamical properties of the airplane are taken into account, for both, airplanes with internal combustion engines and propellers, and airplanes with jet engines. A procedure is presented for the construction of tables from which the flyability of trajectories at a given angle of inclination can be read, together with the corresponding minimum and maximum radii allowed. Sample calculations are shown for the Cessna 182, a Silver Fox like unmanned aerial vehicle, and a F-16 jet airplane.

Keywords: airplane circular trajectory; inclined circular trajectories, airplane equation of motion; circular arc connection; automatic trajectory planning

1. Introduction

This study is a contribution to the endeavor of automatic mission planning for airplanes and in particular for unmanned aerial vehicles (UAVs). Whereas the flight programs of commercial airplanes are usually fairly simple and determined before the airplane takes off, that of UAVs is generally more complex, and very often have to be adapted to unforeseen circumstances during the mission. Thus UAVs should be able to perform on-board trajectory re-planning in response to various events. In order to help realize this task, it is necessary to have at one's disposal mathematical formulas for determining what trajectories this particular airplane can fly and what their relative costs are. It is the purpose of this article to present the derivation of such formulas for inclined circular trajectories.

A common approach to automatic trajectory planning consists in firstly constructing a stick trajectory, that is a continuous sequence of rectilinear segments, and then smoothing the connections between these segments so that the velocity of a point moving on this trajectory would be continuous. Labonté (2011, 2015) analysed the dynamics of airplanes on rectilinear segments inclined at arbitrary angles, and derived necessary and sufficient conditions for engine-propeller driven airplanes to be able to follow such trajectories. Although the corresponding analysis has not yet been done for jet airplanes, it would not be too difficult to do, based on the work about

*Corresponding author, Emeritus Professor, E-mail: gilles.labonte@rmc.ca

propeller airplanes. There are two main approaches for connecting smoothly the rectilinear segments: one uses circular arcs and the other one B-splines. The B-spline approach is described in, among others, Zheng *et al.* (2003), Nikolos *et al.* (2003) and Yang and Sukkarieh (2010). This method has the disadvantage of producing final trajectories that may deviate considerably from the initial stick trajectories. Furthermore, the splines are not easily analysed for their dynamical flyability by airplanes; to our knowledge, no such analysis has yet been done. The first method generalizes, to three dimensions, the work of Dubins (1957) according to which trajectories can be built up from rectilinear and circular segments. This technique has been explained in, among others, Chandler *et al.* (2000), Chitsaz and LaValle (2004), Jia and Vagners (2004), Myung Hwangbo *et al.* (2007), Li Xia *et al.* (2009), Ambrosino *et al.* (2009), Babaei and Mortazavi (2010), Hota and Ghose (2010). In three dimensions, the connecting circular arcs have to lie in inclined planes. Furthermore, these trajectories are very often considered to be flown at constant speed, as is the case in all the references just mentioned.

Notwithstanding the evident importance of such inclined circular trajectories, it is remarkable that no rigorous formulas yet exist to determine whether or not they are compatible with the dynamics of the airplane supposed to fly them. Almost all airplane dynamics manuals discuss circular trajectories in the horizontal plane under the heading of “banked turns”. Many also discuss circular trajectories in the vertical plane as loops, pull-ups or pull-downs. A few have a section on aerobatics where they discuss inverted loops and various turning trajectories such as spirals (see for example, Chapter 3 of Phillips (2004), Chapter 8 of Mair and Birdsall (1992), or Section 15 of Cowley and Levy (1920)), which are actually similar to circular trajectories in an inclined plane. However, we have not found published any complete solution to the equations of motion that would give the position, velocity and acceleration of an airplane, as a function of time, for circular trajectories inclined with an arbitrary angle.

In all the discussion of climbing or descending flights that we have found, except for the vertical loops, the approximation is made that θ_H , the angle of the trajectory with the horizontal plane, is small so that $\cos(\theta_H) \approx 1$. Although this is true for many conventional airplanes for which θ_H is limited to roughly 10° - 15° or less, it is not true for UAVs or high performance jet fighters such as the F-16. UAVs come in a wide range of sizes and agilities and they can fly much more daring maneuvers as inhabited airplanes. For example, some commonly available radio-controlled planes can easily climb at 45° or steeper, as for example, the Carl Goldberg Falcon 56 described by Granelli (2007) and the Hangar 9 Twist 40 described by Horizon Hobby (2004). Therefore, in the present study, we do not make the small angle approximation and the formulas we derive are applicable for any angle of inclination θ_H .

1.1 Assumptions

As remarked in the chapter “Nonuniform Flight” of Von Mises (1945), it is very rare that the equation of motion for a rigid body, with all its six degrees of freedom, can be integrated. Furthermore, it would be very complicated to actually take into account all the aerodynamic forces acting on the different parts of an airplane that is in nonuniform motion, due to its asymmetric attitude with respect to its trajectory. In this same chapter, Von Mises discusses vertical loops and banked horizontal turns and points out that in curved trajectories, “the air reactions must supply, in addition to the centripetal force ..., a rolling, a pitching, and a yawing moment...” After some calculations for the banked turn, he further comments that, under normal conditions, the moments required for maintaining the steady rotation are, after all, unimportant. A similar remark can be

found in Chapter 8 of Mair and Birdsall (1992) in which vertical loops, horizontal banked turns and helicoidal trajectories are discussed. In Section 8.5, they state “that any increase of drag due to the angular velocity of the aircraft and the deflections of the control surfaces can be neglected in comparison with the dominant increase of the lift-dependent drag”. Section 15 of Cowley and Levy (1920) comments similarly that a rigorous treatment of curved flight trajectories would be extremely complicated because of imperfectly known factors related to the variation in aerodynamic forces along the wings, due to their non-symmetric role in the motion. They also assume that “any increase of drag due to the angular velocity of the aircraft and the deflections of its control surfaces can be neglected in comparison with the dominant increase of lift-dependent drag.”

Thus, in the present study, we make the same assumptions that the dynamics involved in the rotations of the airplane about its center of mass, which necessarily occur in the curved motions we examine, are negligible in comparison with those that concern the motion of its center of mass. We also do not take into account the perturbations of the atmosphere and assume that the circular trajectories are small enough that the air density, the air temperature and the weight of the airplane can be considered constant during the motion. Finally, we make ours the remark in the introduction to Chapter “Aircraft Performance” of Phillips (2004) to the effect that the material we present “should be thought of as only a preliminary study of airplane performance. Here, emphasis is placed on obtaining closed-form analytic solutions suitable for preliminary design”.

1.2 Representative airplanes

Our study deals with airplanes with the two types of powerplant: internal combustion engines with propellers and jet engines. We recall that the thrust required T_R on a particular trajectory depends on the configuration of the airplane body, on the manoeuvre it executes and on the state of the atmosphere about it. On the other hand the thrust available T_A depends only on the propulsion system of the airplane. The power P is related to the thrust T by the relation $P=TV_\infty$. As discussed in Chapter 9 of Anderson (2000), for a reciprocating engine-propeller combination, the power available P_A is such that $P_A=\eta P$, with η the propeller efficiency and P the shaft brake power of the engine. P_A is directly proportional to the engine rpm and the air pressure ρ_∞ . At a given air pressure, the power available P_A has a maximum constant value P_{Amax} that corresponds to the engine running at its maximum regime. For fixed pitch propeller and also for constant speed propeller at small speeds, the propeller efficiency η depends on the speed of the airplane. For a jet engine, the thrust available T_A is directly proportional to the air density but can be considered reasonably independent of the speed. At constant air pressure, it has a maximum value T_{Amax} that depends only on the engine.

After having derived the required formulas, we shall illustrate their application with airplanes that have similar properties as the following three well known, very different airplanes:

- the Cessna 182 Skylane,
- a Silver Fox like unmanned aerial vehicle (UAV),
- the Lockheed-Martin F-16 fighter jet.

The values of the characteristic parameters, we use for them, are listed in Appendix A. There may be small differences between some of those parameters and their actual values but they are precise enough for our purpose of illustrating the flight analysis procedure. We have selected these particular three airplanes because they are representative of three different propulsion systems. The thrust of the Cessna 182 is provided by a reciprocating engine with constant speed propeller; that

of the Silver Fox by a reciprocating engine with a fixed pitch propeller, and that of the F-16 by a jet engine.

We recall that the efficiency of the propeller is a function of the advance ratio J , defined as:

$$J = \frac{V_\infty}{ND}$$

in which N is its number of revolution per second and D is its diameter. Thus the maximum power available P_{Amax} will depend on the speed, according to the equation

$$P_{Amax} = \eta(J)P_{max} \quad (1)$$

The dependence of η on J for a constant speed propeller has the general features shown in Fig. 1(a). This curve approximates that given in Cavcar (2004) by the following quadratic expressions

$$\begin{aligned} \eta(J) &= \left[\frac{0.663}{0.640} \right] [J - 0.8]^2 + 0.8 & \forall J \leq 0.8. \\ \eta(J) &= 0.8 & \forall J > 0.8. \end{aligned} \quad (2)$$

The dependence of η on J for a fixed pitch propeller has the general features shown in Fig. 1(b). This curve approximates that given in the Aeronautics Learning Laboratory for Science Technology and Research (ALLSTAR) of the Florida International University (2011) by the following quadratics

$$\begin{aligned} \eta(J) &= -\left[\frac{0.83}{0.49} \right] [J - 0.70]^2 + 0.83 & \forall J \leq 0.7. \\ \eta(J) &= -\left[\frac{0.83}{0.06} \right] [J - 0.70]^2 + 0.83 & \forall J > 0.7. \end{aligned} \quad (3)$$

1.3 Organization of the article

The first sections of this article are valid for all inclined circular trajectories, whether they are traversed at constant speed or not. They start with a mathematical description of such trajectories in terms of the convenient Frenet-Serret frame variables. Formulas for the bank angle, the load factor, the lift coefficient and the thrust required are then obtained and some of their general properties are derived. The implications of the boundedness of these physical parameters are derived for constant speed trajectories, yielding inequalities for the centripetal acceleration and the speed and the inclination angle. The rest of the article deals only with constant speed trajectories for which many inequalities are obtained on the trajectory and flight parameters. Section 7 examines the consequences of the non-negativity requirement for the thrust. Section 8 analyses the constraints that follow from the upper-boundedness of the power available for propeller airplanes. Section 9 presents a similar analysis about the upper-boundedness of the thrust available for jet airplanes. Finally, a systematic procedure for determining the flyability of circular trajectories is presented in the last section. It is illustrated through the construction of tables of possible parameters for flyable trajectories, for the three different types of airplanes mentioned above.

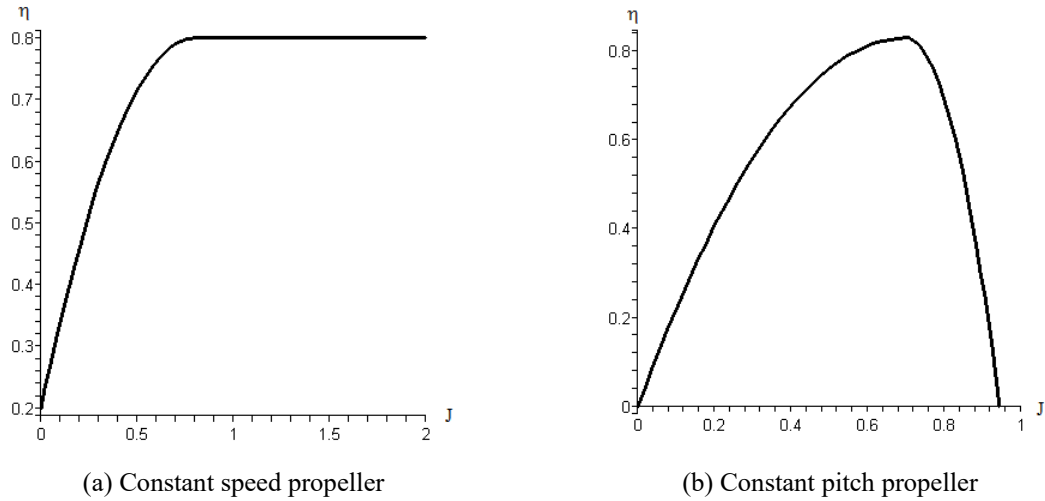


Fig. 1 Typical efficiency factor η as a function of the advance ratio J

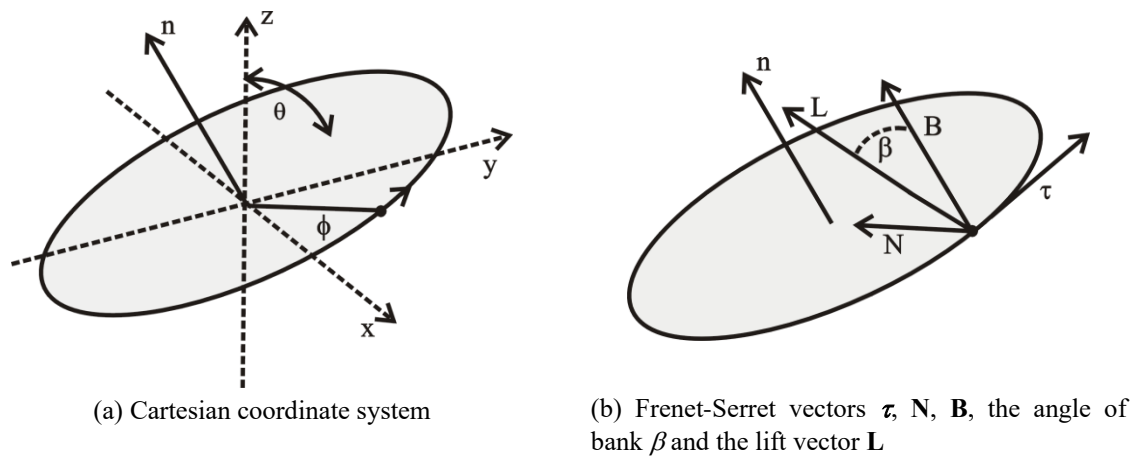


Fig. 2 Parameters used in the description of circular trajectories inclined by an angle θ with respect to the vertical

2. Equation of motion

Let us consider an airplane that flies on a circular trajectory that lies in a plane inclined by an angle θ with respect to the vertical. Fig. 2 represents such a trajectory, for which we have chosen the coordinate axes so that its horizontal diameter is along the x -axis. Let \mathbf{n} represent the unit vector that is normal to the plane in which it lies, then

$$\mathbf{n} = [0, -\cos(\theta), \sin(\theta)].$$

The position of the centre of mass of the airplane, at time t , on the trajectory is given by $\mathbf{x}(t)$:

$$\mathbf{x}(t) = \mathbf{C} + R \mathbf{r} \quad \text{in which}$$

- $\mathbf{r} = [\cos(\phi), \sin(\theta) \sin(\phi), \cos(\theta) \sin(\phi)]$ is the unit radial vector
- $\mathbf{C} = [C_1, C_2, C_3]$ is the position of the centre of the circle,
- R is its radius,
- ϕ is the angle, in the plane of the circular trajectory, which the airplane position vector makes with the x -axis.

Whatever the speed of the airplane on this circular trajectory, ϕ is a monotonically increasing function of t if the trajectory is traversed in the counterclockwise direction around the normal \mathbf{n} and otherwise, it is monotonically decreasing. It is such that $\phi(0)=0$ and $\phi(P)=2\pi$, when P is the period, i.e., the time required to fly around the trajectory. Note that, for counterclockwise motion, the airplane is ascending when $\phi \in [-\pi/2, \pi/2]$ and it is descending when $\phi \in [\pi/2, 3\pi/2]$. For a constant speed trajectory, $\phi = \omega t$, in which ω is a constant $= 2\pi/P$. Its velocity is $\mathbf{v}(t)$

$$\mathbf{v}(t) = \mathbf{x}'(t) = V_\infty \boldsymbol{\tau}$$

where $V_\infty = R \phi'$ and $\boldsymbol{\tau} = [-\sin(\phi), \sin(\theta) \cos(\phi), \cos(\theta) \cos(\phi)]$. $\boldsymbol{\tau}$ is the unit vector tangent to the trajectory. For constant speed trajectories, $V_\infty = R\omega$. For the sake of clarity, we shall hereafter consider that the trajectory is in the counterclockwise direction so that $\phi' > 0$ at all times. We shall use the Frenet-Serret frame of reference that is particularly useful in the description of such trajectories. Fig. 2(b) shows its basis vectors. The unit principal normal vector \mathbf{N} is directed toward the centre of the circle with $\mathbf{N} = -\mathbf{r}$.

The acceleration of the airplane is: $\mathbf{a}(t) = \mathbf{v}'(t) = R \phi'' \boldsymbol{\tau} + \frac{V_\infty^2}{R} \mathbf{N}$. For constant speed trajectories, this reduces to $\mathbf{a}(t) = \frac{V_\infty^2}{R} \mathbf{N}$. The unit binormal vector \mathbf{B} is simply the vector \mathbf{n} .

2.1 The forces at play

The physical forces at play are

- the lift \mathbf{L} ,
- the gravitational force $\mathbf{W} = -W \mathbf{k}$, with $\mathbf{k} = [0, 0, 1]$,
- the longitudinal force that corresponds to the thrust produced by the propulsion system T minus the drag D ; its value is then $(T-D)\boldsymbol{\tau}$.

The lift \mathbf{L} is perpendicular to the velocity of the airplane and its bank angle β , is measured with respect to the normal to the plane of the trajectory, \mathbf{L} can be written as:

$$\mathbf{L} = L \cos(\beta) \mathbf{n} + L \sin(\beta) \mathbf{N}(t)$$

Fig. 2(a) shows how the bank angle is defined; it can take any value, corresponding to the airplane flying in any possible attitude on the trajectory. Newton's equation of motion is

$$\frac{W}{g} \mathbf{a} = \mathbf{L} + \mathbf{W} + (T-D) \boldsymbol{\tau} \quad (4)$$

The \mathbf{n} , \mathbf{N} and $\boldsymbol{\tau}$ components of this equation are respectively

$$L \cos(\beta) = W \sin(\theta) \quad (5)$$

$$L \sin(\beta) = \frac{WV_{\infty}^2}{gR} - W \cos(\theta) \sin(\phi), \quad (6)$$

$$T = D + \frac{WR}{g} \phi'' + W \cos(\theta) \cos(\phi) \quad (7)$$

We define A_c , the centripetal acceleration in units of g as

$$A_c = \frac{V_{\infty}^2}{gR} - \cos(\theta) \sin(\phi). \quad (8)$$

Eq. (6) can then be written as

$$L \sin(\beta) = W A_c. \quad (9)$$

3. Bank angle

3.1 Vertical loops

In a vertical loop, $\theta=0$ and Eq. (5) then implies that $\cos(\beta)=0$ so that either $\beta=\pi/2$ or $\beta=-\pi/2$ everywhere along the trajectory. The first case corresponds to the loop usually performed in aerobatics shows, in which the airplane is upside up at the bottom of the loop and upside down at the top. The case with the angle of bank $\beta=-\pi/2$, corresponds to an “inverted loop” in which the airplane is upside down at the bottom of the loop and upside up at the top.

3.2 Non-vertical trajectories

When $\theta \neq 0$, we divide Eq. (9) by Eq. (5) and obtain the following equation for the bank angle

$$\tan(\beta) = \frac{A_c}{\sin(\theta)}. \quad (10)$$

This equation indicates that all airplanes must bank by the same angle β in order to travel with the same speed V_{∞} on this circular trajectory, a fact that generalises a well-known property of horizontal circular trajectories. It also shows that the bank angle will generally vary along the trajectory. It should be noted that, because the right-hand-side (RHS) of Eq. (5) is always positive when $\theta \neq 0$, its left-hand-side (LHS) cannot be null at any point of the trajectory. Thus, L and $\cos(\beta)$ must always keep the same sign, either positive or negative, at every point of the trajectory, and this sign has to be the same one for both of them. According to Eq. (8), A_c is always positive when $\phi = 0$, thus, $\tan(\beta)$ is positive and both $\sin(\beta)$ and $\cos(\beta)$ must then have the same sign at this point. If this sign is positive, because $\cos(\beta)$ has to remain positive everywhere, the angle of bank β has to remain in the interval $(-\pi/2, \pi/2)$, and the airplane has to keep flying upside up for the whole trajectory. If $\cos(\beta)$ is negative the angle of bank has to remain in the interval $(\pi/2, 3\pi/2)$, with the airplane flying upside down, on the whole trajectory. Thus,

$$\sin(\beta) = \varepsilon \frac{A_c}{\sqrt{\sin^2(\theta) + A_c^2}} \quad \cos(\beta) = \varepsilon \frac{\sin(\theta)}{\sqrt{\sin^2(\theta) + A_c^2}} \quad (11)$$

with $\varepsilon=+1$ in the first case and -1 in the second one. According to Eq. (10), if the lift vector points toward the region above the trajectory and A_c changes sign, then $\sin(\beta)$ will change sign, indicating that the lift vector will now point away from this region, and vice versa.

3.3 Trajectories at constant speed

We note that the centripetal acceleration A_c is symmetrical through reflection in the vertical plane that passes through $\phi=\pi/2$ and $\phi=3\pi/2$. Thus the bank angle also has this symmetry. Its minimum value is at $\phi=\pi/2$ and its maximum value is at $\phi=3\pi/2$. There would be sections of the trajectory on which the bank angle would change sign as the centripetal acceleration A_c would change sign. However, it will be shown in Section 7 that, for trajectories at constant speed, it is necessary to have $\frac{V_\infty^2}{gR} > \cos(\theta)$ so that A_c will always be positive. Thus, the bank angle will keep the same sign for the whole trajectory. Fig. 3(a) shows how the bank angle varies with ϕ , for $\varepsilon=1$, for the Cessna 182, when $\theta=\pi/6$ and $V_\infty^2 / gR = 1.5 \cos(\theta)$.

4. Load factor

According to Eq. (5), the load factor is

$$n = \frac{L}{W} = \varepsilon \sqrt{\sin^2(\theta) + A_c^2} \tag{12}$$

with ε as in Eq. (11), and, as is the case for L , the load factor keeps the same sign on the whole trajectory, which is that of the bank angle. Fig. 3(b) shows how the load factor varies with ϕ , for $\varepsilon=1$, for the Cessna 182, when $\theta=\pi/6$ and $V_\infty^2 / gR = 1.5 \cos(\theta)$.

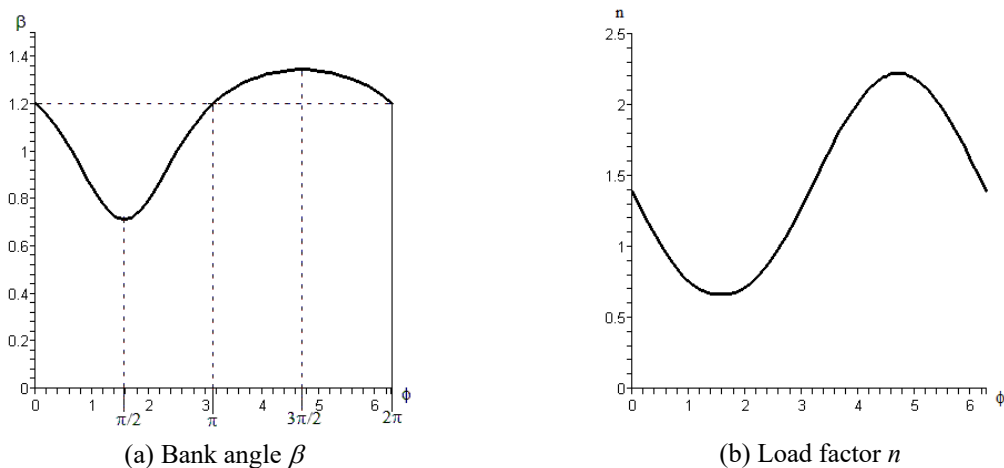


Fig. 3 Bank angle and load factor as functions of the position angle ϕ that varies from 0 to 2π when $\theta=\pi/6$ and $V_\infty^2 / gR = 1.5 \cos(\theta)$

n is bounded such that

$$n_{\min} \leq n \leq n_{\max} \quad (13)$$

thus, from Eqs. (8), (12) and (13), one can deduce that

$$\left[\frac{V_{\infty}^2}{gR} - \cos(\theta) \sin(\phi) \right]^2 \leq n_{\lim}^2 - \sin^2(\theta), \quad \text{with } n_{\lim} = \begin{cases} n_{\max} & \text{if } \varepsilon = +1 \\ n_{\min} & \text{if } \varepsilon = -1 \end{cases}. \quad (14)$$

Again, for the sake of clarity, we shall hereafter consider trajectories on which $\varepsilon = +1$; the case with $\varepsilon = -1$ can be dealt with the same way.

4.1 Horizontal trajectories

In a horizontal trajectory, $\theta = \pi/2$, so that $A_c = \frac{V_{\infty}^2}{gR}$ and Eq. (12) becomes simply $n = \sec(\beta)$, which is an equation found in most textbooks on airplane dynamics, as for example in Chapter 2 of Stengell (2004). For upside-up flight, Ineq. (14) yields the following upper bound for the radius of the trajectory: $R \geq \frac{V_{\max}^2}{g \sqrt{n_{\max}^2 - 1}}$, in which V_{\max} is the maximum speed of the airplane on the circular trajectory.

4.2 Vertical loops

For vertical loops, $\theta = 0$ and $A_c = \frac{V_{\infty}^2}{gR} - \sin(\phi)$. The load factor is $n = \varepsilon A_c$ so that there is a restriction on R that results from the constraints: $\text{Max}\{A_c\} \leq n_{\max}$ and $\text{Min}\{A_c\} \geq n_{\min}$, in which the maximum and minimum are calculated over the trajectory. These values depend on the value of ϕ' . We note that A_c is always positive at the bottom of the trajectory where $\phi = -3\pi/2$. Thus, in inverted loops, the load factor is always negative near this point where the airplane is upside down. When discussing vertical loops, Von Mises (1945) points out that the inverted loop is a maneuver of extreme difficulty and danger, due to this large negative load when the airplane is inverted. He interestingly remarks that it is often forbidden to accomplish this aerobatics figure when a pilot is inside the plane, except under strict precautions and regulations.

4.3 Constant speed trajectories at arbitrary inclinations

We note that Ineq. (14) holds $\forall \phi$ if and only if it holds when its LHS is maximum. This occurs at $\phi = -\pi/2$; thus Ineq. (14) implies an upper bound on the average centripetal acceleration

$$\frac{V_{\infty}^2}{gR} \leq -\cos(\theta) + \sqrt{n_{\max}^2 - \sin^2(\theta)}. \quad (15)$$

5. Lift coefficient

The lift coefficient has to be bounded as follows

$$C_{Lmin} \leq C_L \leq C_{Lmax} . \quad (15)$$

When the expression for $\sin(\beta)$ given in Eq. (11), is substituted in Eq. (9), one obtains

$$C_L = \frac{2Wn}{\rho_\infty S V_\infty^2} = \frac{2\varepsilon W}{\rho_\infty S V_\infty^2} \sqrt{\sin^2(\theta) + A_c^2} . \quad (16)$$

Thus Ineqs. (15) can be rewritten as: $\frac{\rho_\infty S C_{Lmin} V_\infty^2}{2W} \leq n \leq \frac{\rho_\infty S C_{Lmax} V_\infty^2}{2W}$, which has the same form as Ineq. (13) and can therefore be analysed in the same way. For constant speed flight, in which the airplane is flying upside up, it thus yields the constraint

$$\frac{V_\infty^2}{gR} \leq -\cos(\theta) + \sqrt{\left[\frac{\rho_\infty S C_{Lmax} V_\infty^2}{2W} \right]^2 - \sin^2(\theta)} . \quad (17)$$

A condition that can be satisfied only if

$$V_\infty \geq \sqrt{\frac{2W}{\rho_\infty S C_{Lmax}}} . \quad (18)$$

Since, according to Eq. (16), C_L is directly proportional to n ; it varies in the same way as n along the trajectory. Thus, the curves shown in Fig. 4 are proportional to those representing C_L on the trajectories considered. The upper bound on the average centripetal acceleration that corresponds to Ineq. (17) is represented by the meshed surface in Fig. 4; the grey region below represents the allowed average centripetal accelerations.

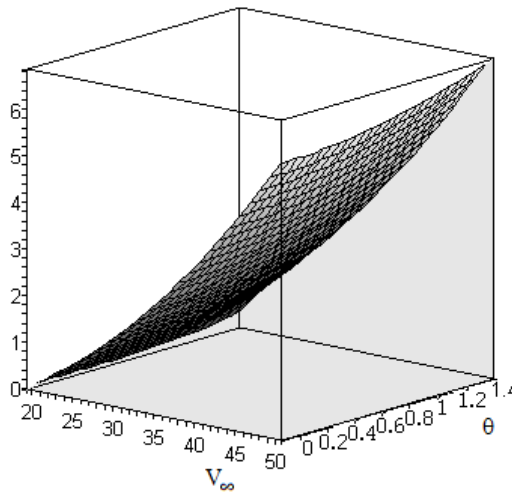


Fig. 4 Region of allowed average centripetal acceleration, shown in grey, for the Cessna 182

6. Thrust and power required

Upon replacing the drag D by its value in Eq. (7), one obtains the following expression for the thrust required T_R

$$T_R = \frac{1}{2} \rho_\infty S \left[C_{D0} + \frac{C_L^2}{\pi e AR} \right] V_\infty^2 + \frac{WR}{g} \phi' + W \cos(\theta) \cos(\phi).$$

When C_L is replaced by its value, given in Eq. (16), one obtains

$$T_R = \bar{C}_{D0} V_\infty^2 + \frac{\Gamma}{V_\infty^2} \left\{ \sin^2(\theta) + \left[\frac{V_\infty^2}{gR} - \cos(\theta) \sin(\phi) \right]^2 \right\} + \frac{WR}{g} \phi' + W \cos(\theta) \cos(\phi) \quad (19)$$

in which

$$\bar{C}_{D0} = \frac{1}{2} \rho_\infty S C_{D0} \quad \text{and} \quad \Gamma = \frac{2W^2}{\pi e AR \rho_\infty S}. \quad (20)$$

The power required for the motion is $P_R = V_\infty T_R$. Whatever the speed, the thrust is always bounded since the power output of the motor is limited. For propeller airplanes, this bound is expressed in terms of the maximum power available P_{Amax} as

$$P_R \leq P_{Amax}. \quad (21)$$

For jet airplanes, if the maximum thrust available is denoted by T_{Amax} , the limit on the thrust implies

$$T_R \leq T_{Amax}. \quad (22)$$

7. Non-negativity of the thrust at constant speed

For constant speed trajectories, T_R must remain non-negative on the whole trajectory since a negative thrust implies a deceleration. We shall examine this constraint in the present section. We note that, in the expression for T_R , given in Eq. (19), all the terms, except the last one are symmetrical about a vertical plane passing through the lowest and the highest points of the trajectory. This last term is positive during the ascending phase of the trajectory and negative in the descending phase. We then only have to ensure non-negativity for the descending phase, where $\cos(\phi) < 0$. It is then required that $\forall \phi \in (\pi/2, 3\pi/2)$

$$\bar{C}_{D0} V_\infty^2 + \frac{\Gamma}{V_\infty^2} \left\{ \sin^2(\theta) + \left[\frac{V_\infty^2}{gR} - \cos(\theta) \sin(\phi) \right]^2 \right\} + W \cos(\theta) \cos(\phi) \geq 0. \quad (23)$$

Fig. 5(a) shows the thrust required as a function of the angle ϕ , for the Cessna 182 to fly on a circular trajectory inclined by 10 degrees with the horizontal, with radius $R=100$ m, at a speed of 25 m/s. As can be seen, there are values of ϕ , when the airplane is descending, at which the thrust would be negative so that such a trajectory would not be possible for this plane. However, on the

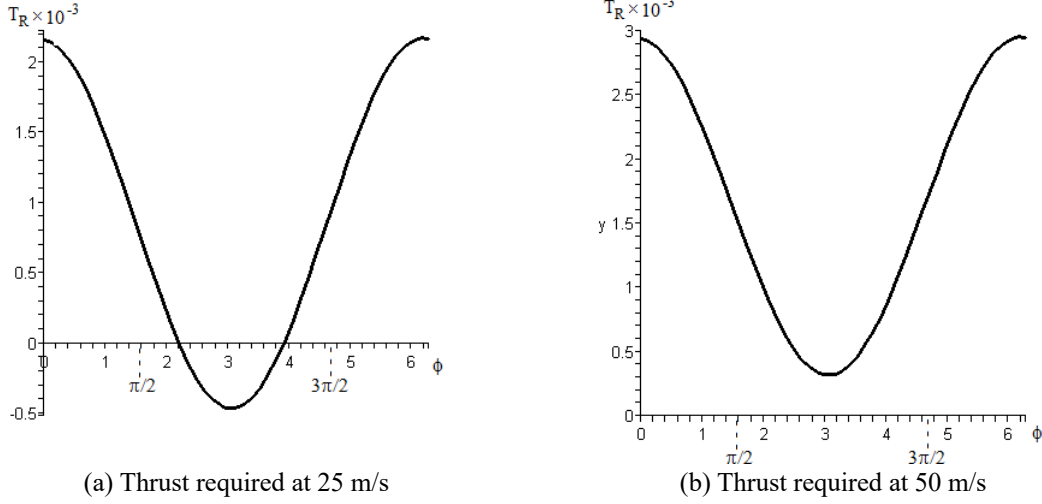


Fig. 5 Thrust required as a function of the angle ϕ , for the Cessna 182 to fly on a circular trajectory inclined by 10 degrees with the horizontal, with radius $R=100$ m

same trajectory, with a speed of 50 m/s, the thrust required would remain positive, as can be seen in Fig. 5(b).

We remark that for trajectories in an horizontal plane, $\theta=\pi/2$ so that Ineq. (23) is always satisfied. We thus only have to examine the case in which $\theta\neq\pi/2$. In analysing Ineq. (23), it is useful to remember that V_∞ and $\frac{V_\infty^2}{gR}$ are two distinct variables. Upon multiplying Ineq. (23) by V_∞^2 , there results

$$Q(\phi) + \Gamma \left[\frac{V_\infty^2}{gR} - \cos(\theta) \sin(\phi) \right]^2 \geq 0 \quad (24)$$

with

$$Q(\phi) = \bar{C}_{D0} V_\infty^4 + W \cos(\theta) \cos(\phi) V_\infty^2 + \Gamma \sin^2(\theta). \quad (25)$$

Let us define U

$$U(V_\infty, \theta) = - \frac{[\bar{C}_{D0} V_\infty^4 + \Gamma \sin^2(\theta)]}{W V_\infty^2 \cos(\theta)}, \quad (26)$$

such that if

$$U(V_\infty, \theta) \leq -1, \text{ then } Q(\phi) \geq 0 \forall \phi, \quad (27)$$

and if $U(V_\infty, \theta) > -1$, then $Q(\phi) < 0 \forall \phi$ such that $\cos(\phi) < \cos(\phi_1)$ with $\cos(\phi_1) = U(V_\infty, \theta)$ and $\phi_1 \in [\pi/2, \pi]$. Such ϕ 's are then in the interval $\phi \in (\phi_1, 2\pi - \phi_1)$. In the rest of the interval $[\pi/2, 3\pi/2]$, $Q(\phi) \geq 0 \forall \phi$, with $Q(\phi) = 0$ at $\phi = \phi_1$ and $2\pi - \phi_1$. Fig. 6(a) shows, in grey, the

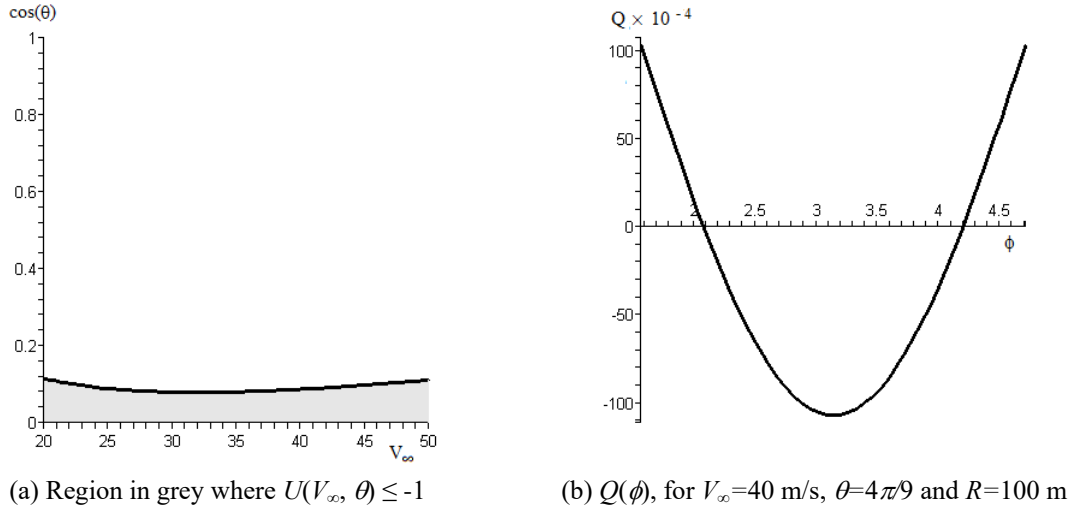


Fig. 6 Some characteristic functions related to the thrust required

region of the $(V_\infty, \cos(\theta))$ plane in which $U(V_\infty, \theta) \leq -1$. Fig. 6(b) shows Q as a function of ϕ for the Cessna 182, on the trajectory inclined at 10° with the horizontal, with radius $R=100$ m, at the speed of 40 m/s. In that case, $\phi_1=2.084$.

We now examine further Ineq. (24) for the angles ϕ such that $Q(\phi) < 0$. The LHS of Ineq. (24) can then be factorized to yield

$$\left\{ \sqrt{\Gamma} \left[\frac{V_\infty^2}{gR} - \cos(\theta) \sin(\phi) \right] + \sqrt{-Q(\phi)} \right\} \left\{ \sqrt{\Gamma} \left[\frac{V_\infty^2}{gR} - \cos(\theta) \sin(\phi) \right] - \sqrt{-Q(\phi)} \right\} \geq 0. \quad (28)$$

Consequently, we shall consider the following two situations that correspond to the sign of the factor in square brackets in this inequality.

Case 1: ϕ is such that $\left[\frac{V_\infty^2}{gR} - \cos(\theta) \sin(\phi) \right] \leq 0$.

This conditions requires that

$$\frac{V_\infty^2}{gR \cos(\theta)} \leq 1 \quad \text{with } \phi \leq \phi_2 \text{ where } \sin(\phi_2) = \frac{V_\infty^2}{gR \cos(\theta)}. \quad (29)$$

There are such ϕ 's in the interval $(\phi_1, 2\pi - \phi_1)$ if and only if $\phi_2 > \phi_1$. Thus, the interval to consider here is $I = (\phi_1, \phi_2)$. In this interval, Ineq. (28) reduces to

$$F_1(\phi) = \sqrt{\Gamma} \left[\frac{V_\infty^2}{gR} - \cos(\theta) \sin(\phi) \right] + \sqrt{-Q(\phi)} \leq 0. \quad (30)$$

This inequality will hold $\forall \phi \in I$ if and only if it holds for the maximum value of $F_1(\phi)$ in this interval. This value will occur either at the limit points of the interval I or at the critical points at

which $F_1'(\phi) = 0$. This equation for critical points reduces to

$$WV_\infty^2 \sin(\phi) = 2\sqrt{\Gamma} \cos(\phi) \sqrt{-Q(\phi)}.$$

Since its RHS is negative, this equation requires $\sin(\phi)$ to be negative. However, this is never the case for $\phi \in I$; thus F_1 has no local maximum in I , and it is maximum at one of the end points of I . It is straightforward to see that this maximum is $F_1(\phi_2) = \sqrt{-Q(\phi_2)}$. This is positive and therefore Ineq. (30) is not satisfied at this point, and we must conclude that it is necessary to have

$$\frac{V_\infty^2}{gR} > \cos(\theta) \tag{31}$$

so that Case 1 does not occur.

Case 2: ϕ is such that $\left[\frac{V_\infty^2}{gR} - \cos(\theta) \sin(\phi) \right] > 0$.

Because of Ineq. (31), this is true for all ϕ 's so that the interval to consider is $I = (\phi_1, 2\pi - \phi_1)$. Ineq. (28) then reduces to

$$F_2(\phi) = \sqrt{\Gamma} \left[\frac{V_\infty^2}{gR} - \cos(\theta) \sin(\phi) \right] - \sqrt{-Q(\phi)} \geq 0. \tag{32}$$

This inequality will hold $\forall \phi \in I$ if and only if it holds when $F_2(\phi)$ is minimum in this interval. This minimum value will occur either at the limit points of the interval I or at critical points where $F_2'(\phi) = 0$. This equation for critical points reduces to

$$WV_\infty^2 \sin(\phi) = -2\sqrt{\Gamma} \cos(\phi) \sqrt{-Q(\phi)}. \tag{33}$$

Since the RHS of this equation is positive, $\sin(\phi)$ must also be positive, so that the critical points must be in the sub-interval I_1 of I that ends at $\phi = \pi$. Upon squaring Eq. (33), one obtains the following cubic equation for $\cos(\phi)$ that can readily be solved:

$$P_3(\cos(\phi)) = 0$$

with

$$P_3(x) = \left[4\Gamma WV_\infty^2 \cos(\theta) \right] x^3 + \left[4\Gamma \bar{C}_{D0} V_\infty^4 - W^2 V_\infty^4 + 4\Gamma^2 \sin^2(\theta) \right] x^2 + W^2 V_\infty^4 \tag{34}$$

Since the coefficients of x^3 and of 1 in $P_3(x)$ are positive, P_3 has only one negative real root. Let r_- represent this root. If r_- is in the interval $[-1, 1]$ and if $\phi_3 = \cos^{-1}(r_-)$ is in (ϕ_1, π) , then ϕ_3 is a critical point for F_2 , otherwise F_2 has no critical point in the interval of interest. The values of F_2 at the ends of the interval are:

$$F_2(\phi_1) = \sqrt{\Gamma} \left[\frac{V_\infty^2}{gR} - \cos(\theta) \sin(\phi_1) \right] \quad \text{and} \quad F_2(2\pi - \phi_1) = \sqrt{\Gamma} \left[\frac{V_\infty^2}{gR} + \cos(\theta) \sin(\phi_1) \right]$$

which are both positive because of Ineq. (31). There then remains only to ensure that Ineq. (32)

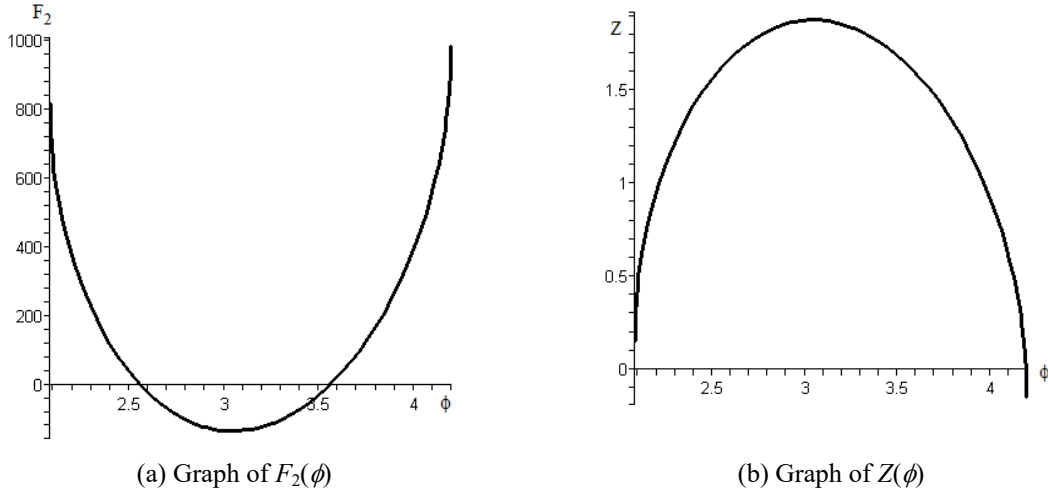


Fig. 7 Some functions related to the thrust required by the Cessna 182, when $V_\infty=40$ m/s, $\theta=4\pi/9$ and $R=100$ m

holds at the critical point, which requires that

$$\frac{V_\infty^2}{gR} \geq Z(\phi_3) \text{ if } \phi_3 \in (\phi_1, \pi) \tag{35}$$

with

$$Z(\phi) = \cos(\theta) \sin(\phi) + \sqrt{\frac{-Q(\phi)}{\Gamma}}. \tag{36}$$

Fig. 7(a) shows the graph of $F_2(\phi)$, for ϕ in the interval $(\phi_1, 2\pi-\phi_1)$, for the Cessna 182, when $V_\infty=40$ m/s, $\theta=4\pi/9$ and $R=100$ m. Fig. 7(b) shows the graph of $Z(\phi)$ in the same interval, for the same flight. We note that Z is an increasing function of $\cos(\theta)$; thus its maximum value can be increased or decreased by decreasing or increasing θ . In this flight, the RHS of Ineq. (35) is 1.878.

8. Upper bound on the power for propeller airplanes

For a trajectory to be flyable, it is necessary that the power the airplane requires does not exceed the power its powerplant can provide. Ineq. (21) expresses this constraint; we shall now derive necessary and sufficient conditions for this inequality to hold. Upon substituting the expression for T_R from Eq. (19), and multiplying Ineq. (21) by V_∞ , there results the inequality

$$Q(\phi) - P_{Amax}(V_\infty) V_\infty + \Gamma \left[\frac{V_\infty^2}{gR} - \cos(\theta) \sin(\phi) \right]^2 \leq 0 \quad \forall \phi. \tag{37}$$

Fig. 8 shows the power required P_R by the Cessna 182 to fly the trajectory at 10° with the horizontal, speed $V_\infty=50$ m/s and radius $R=100$ m, together with the maximum power available P_{Amax} . As can be seen the Cessna has enough power to fly this trajectory.

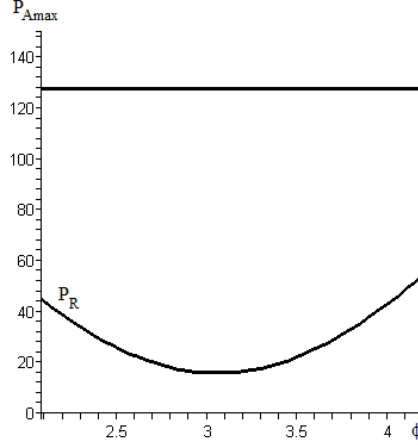


Fig. 8 Power required P_R by the Cessna 182 to fly the trajectory at 10° with the horizontal, speed $V_\infty=50$ m/s and radius $R=100$ m, together with the maximum power available P_{Amax}

At the beginning of Section 5, we remarked that the power required in the descending section of the trajectory is always smaller than that required in the ascending section. Thus we only have to ensure that Ineq. (37) holds in the ascending section, that is for $\phi \in [-\pi/2, \pi/2]$, in order to ensure that it holds over the whole trajectory. For Ineq. (37) to hold, it is necessary that $Q(\phi) - P_{Amax}(V_\infty)V_\infty \leq 0 \forall \phi$, that is

$$\bar{C}_{D0}V_\infty^4 + W \cos(\theta) \cos(\phi) V_\infty^2 - P_{Amax}(V_\infty)V_\infty + \Gamma \sin^2(\theta) \leq 0 \quad \forall \phi. \quad (38)$$

This inequality will hold if and only if it holds when its LHS is maximum. This occurs at $\phi=0$ so that, one needs

$$Q_A(V_\infty, \theta) \leq 0, \quad \text{with } Q_A(V_\infty, \theta) = \bar{C}_{D0}V_\infty^4 + W \cos(\theta) V_\infty^2 - P_{Amax}(V_\infty)V_\infty + \Gamma \sin^2(\theta). \quad (39)$$

This inequality would be solvable in terms of V_∞ if $P_{Amax}(V_\infty)$ could be approximated by quadratic functions of V_∞ as we did in Eqs. (1), (2) and (3). However, we do not know whether that would be a valid approximation in general, so instead, we examine Ineq. (39) from the point of view that Q_A is a quadratic function of $\cos(\theta)$. As such, it corresponds to a downward concave parabola.

Its discriminant is

$$\Delta = W^2 V_\infty^4 + 4\Gamma \left\{ \bar{C}_{D0} V_\infty^4 - P_{Amax}(V_\infty) V_\infty + \Gamma \right\}. \quad (40)$$

If $\Delta \leq 0$, Q_A either has no real roots or has a double root and then Ineq. (39) would be satisfied for all values of θ . However, for the airplanes we considered as examples, Δ is always positive, being always greater than 10^6 . We must then examine more in details the case in which $\Delta > 0$. The two roots of Q_A are then

$$s_\pm = \frac{I}{2\Gamma} \left[W V_\infty^2 \pm \sqrt{\Delta} \right]. \quad (41)$$

and Ineq. (39) will be satisfied if either

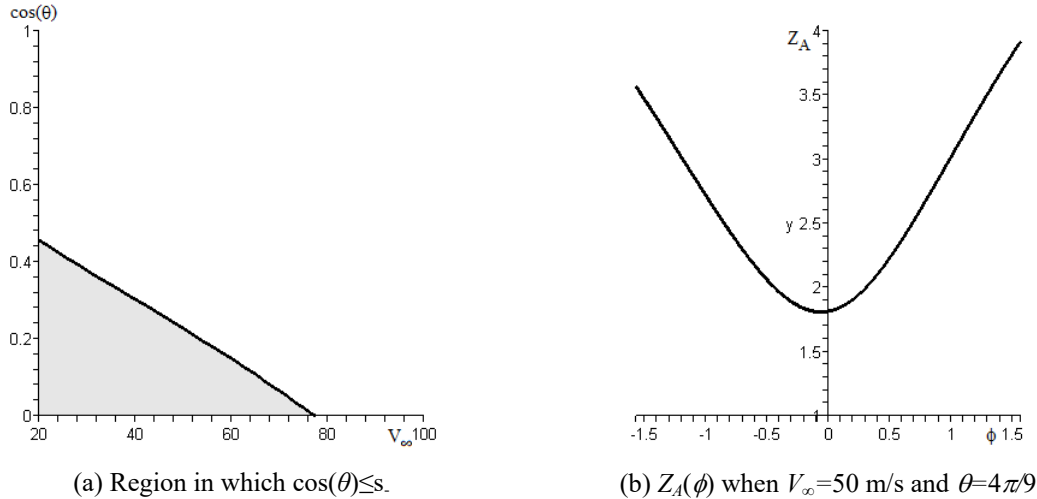


Fig. 9 Some functions related to the power required by the Cessna 182

$$\cos(\theta) \leq s_- \text{ or } \cos(\theta) \geq s_+ \tag{42}$$

This inequality yields a constraint on the possible values of the speed V_∞ and the angle θ . Again, for all the airplanes we considered as examples, $WV_\infty^2/2\Gamma > 1$ so that $s_+ > 1$ and therefore, there are no θ satisfying the second inequality of Ineqs. (42). Thus, the first inequality of Ineqs. (42) must be satisfied. Fig. 9(a) shows in grey the regions of the (V_∞, θ) plane in which it holds, that is, in which $Q_A(V_\infty, \theta) \leq 0$. Given Ineqs. (31), and (38), Ineq. (37) will be satisfied if and only if

$$\frac{V_\infty^2}{gR} \leq Z_A(\phi) \quad \forall \phi \tag{43}$$

with

$$Z_A(\phi) = \cos(\theta) \sin(\phi) + \sqrt{\frac{P_{Amax}(V_\infty)V_\infty - Q(\phi)}{\Gamma}} \tag{44}$$

Fig. 9(b) shows $Z_A(\phi)$ for the Cessna 182, when $\theta=4\pi/9$ and $V_\infty=50$. We note that Ineq. (43) will hold if and only if it holds when Z_A is minimum.

The minimum of Z_A will occur at one of the extremities of the interval $[-\pi/2, \pi/2]$ or at a critical point at which its derivative is null. We note that it is always true that $Z_A(-\pi/2) < Z_A(\pi/2)$. Upon looking for the critical points, one sees that they can exist only where $\sin(\phi) < 0$, that is for $\phi \in (-\pi/2, 0)$, and they should satisfy the equation

$$P_3(\cos(\phi)) - 4\Gamma P_{Amax}(V_\infty)V_\infty \cos^2(\phi) = 0 \tag{45}$$

where P_3 is the same third degree polynomial as defined in Eq. (34). Note that Ineq. (38) ensures that the coefficient of $\cos^2(\phi)$, on the LHS of Eq. (45), is negative. Therefore, the third degree

polynomial in $\cos(\phi)$ on the LHS of Eq. (45) has either no positive real roots or two positive real roots. Let then Φ_r represent the set, which may be empty, of angles in the interval $(-\pi/2, 0)$ that correspond to the roots in $[0, 1]$. Then

$$\frac{V_\infty^2}{gR} \leq \text{Min}\{Z_A(-\pi/2), A\} \quad \text{with} \quad A = \text{Min}_{\Phi_r} Z_A(\phi). \quad (46)$$

9. Upper bound on the thrust for jet airplanes

For jet airplanes, the upper bound on the thrust available corresponds to Ineq. (22). We now derive necessary and sufficient conditions to ensure that this inequality holds. With the value of T_R given in Eq. (19), Ineq. (22) can be written as

$$Q(\phi) - T_{Amax} V_\infty^2 + \Gamma \left[\frac{V_\infty^2}{gR} - \cos(\theta) \sin(\phi) \right]^2 \leq 0 \quad \forall \phi. \quad (47)$$

The analysis of this inequality follows closely that of Ineq. (37). Again, because the thrust required in the descending section of the trajectory is always smaller than that in the ascending section, it suffices to ensure that Ineq. (47) holds $\forall \phi \in [-\pi/2, \pi/2]$. This inequality requires that $Q(\phi) - T_{Amax} V_\infty^2 \leq 0 \forall \phi$, i.e.

$$\bar{C}_{D0} V_\infty^4 + W \cos(\theta) \cos(\phi) V_\infty^2 - T_{Amax} V_\infty^2 + \Gamma \sin^2(\theta) \leq 0 \quad \forall \phi. \quad (48)$$

This condition will hold if and only if it holds when its LHS is maximum, i.e., when

$$\bar{C}_{D0} V_\infty^4 + [W \cos(\theta) - T_{Amax}] V_\infty^2 + \Gamma \sin^2(\theta) \leq 0. \quad (49)$$

This inequality yields constraints on the possible values of the speed V_∞ and the angle of inclination θ . For it to hold, it is necessary that the coefficient of V_∞^2 be negative because all the other terms on its LHS are positive, thus it is required that

$$\cos(\theta) < \frac{T_{Amax}}{W}, \quad (50)$$

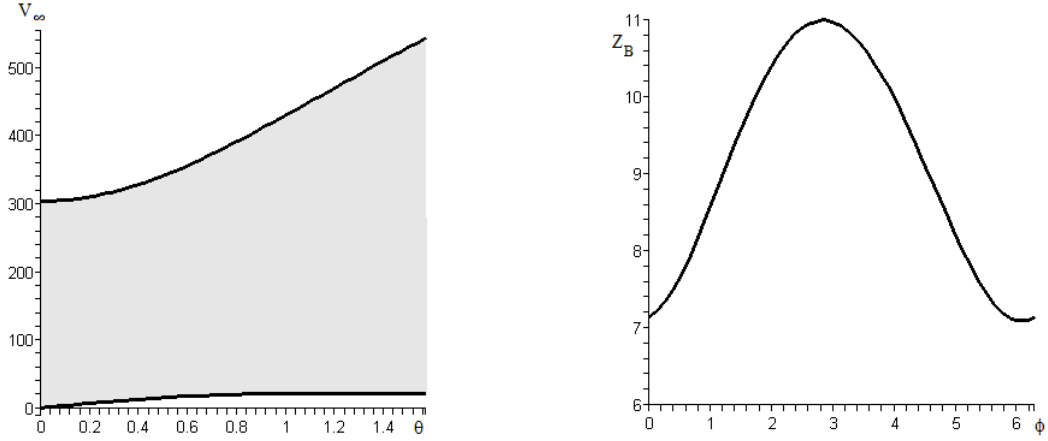
For the F-16 jet airplane, this inequality holds for all θ 's since its RHS is larger 1. Ineq. (49) can then hold only if the discriminant of the quadratic polynomial in V_∞^2 on its LHS is non-negative, i.e.

$$T_{Amax} - W \cos(\theta) - 2\sqrt{\bar{C}_{D0}\Gamma} \sin(\theta) \geq 0. \quad (51)$$

This inequality is a constraint on θ that can be rewritten as

$$\sin(\alpha + \theta) \leq \frac{T_{Amax}}{\sqrt{4\bar{C}_{D0}\Gamma + W^2}} \quad \text{with} \quad \tan(\alpha) = \frac{W}{2\sqrt{\bar{C}_{D0}\Gamma}} \quad (52)$$

For the F-16 jet airplane, this inequality also holds for all θ 's since its RHS is larger 1. If Ineqs. (50) and (51) hold, then Ineq. (49) will hold $\forall V_\infty$, such that



(a) Region, in grey, of the speeds allowed for various values of θ

(b) $Z_B(\phi)$ for $\theta_H=30^\circ$ and $V_\infty=200$ m/s

Fig. 10 Some functions related to the thrust required by the F-16

$$V_-^2 \leq V_\infty^2 \leq V_+^2. \quad (53)$$

where V_\pm^2 are the two roots of the quadratic polynomial in V_∞^2 on the LHS of Ineq. (49), which are

$$V_\pm^2 = \frac{I}{2C_{D0}} \left\{ T_{Amax} - W \cos(\theta) \pm \sqrt{[T_{Amax} - W \cos(\theta)]^2 - 4C_{D0}\Gamma \sin^2(\theta)} \right\}. \quad (54)$$

Fig. 10(a) shows, in grey, the region of allowed speeds for the different values of the angle of inclination θ , according to Ineq. (53). Once Ineq. (48) is ensured to hold, Ineq. (47) will be satisfied if and only if

$$\frac{V_\infty^2}{gR} \leq \underset{\forall \phi}{\text{Min}} Z_B(\phi) \quad (55)$$

with

$$Z_B(\phi) = \cos(\theta) \sin(\phi) + \sqrt{\frac{T_{Amax} V_\infty^2 - Q(\phi)}{\Gamma}} \quad (56)$$

Fig. 10(b) shows the graph of Z_B as a function of $\phi \in [0, 2\pi]$ when the angle of inclination with the horizontal is $\theta_H=30^\circ$ and the speed is $V_\infty=200$ m/s. The minimum of Z_B will occur at one of the extremities of the interval $[-\pi/2, \pi/2]$ or at one of its critical points where its derivative vanishes. Such points occur at ϕ 's that such $\sin(\phi) < 0$, so that ϕ must be in $(-\pi/2, 0)$, and such that

$$P_3(\cos(\phi)) - 4\Gamma T_{Amax} V_\infty^2 \cos^2(\phi) = 0. \quad (57)$$

where P_3 is the same third degree polynomial as defined in Eq. (34). Note that Ineq. (48) ensures that the coefficient of $\cos^2(\phi)$ in the third degree polynomial in $\cos(\phi)$, on the LHS of Eq. (57), is

negative. Therefore, this polynomial has either no positive real roots or two positive real roots. Let then Φ_r represent the set, which may be empty, of angles in the interval $(-\pi/2, 0)$ that correspond to the roots in $[0, 1]$. Then

$$\frac{V_\infty^2}{gR} \leq \text{Min}\{Z_B(-\pi/2), B\} \quad \text{with} \quad B = \text{Min}_{\Phi_r} Z_B(\phi). \quad (58)$$

10. Examples of flyability analysis

We have obtained many conditions for the flyability of inclined circular trajectories at constant speed. We have not been able to solve all of them together and obtain ranges of parameters that are suitable for a particular airplane. Nevertheless, It is not difficult to devise a procedure that allows to test whether trajectories are flyable at a given speed and inclination. Such tables can be produced for any angle of inclination θ . With this approach, one can produce tables of parameters of flyable trajectories; such a procedure could consist of the following steps.

1. Use Ineq. (18), which expresses the upper-boundedness of the lift coefficient, to obtain a lower bound on the speed V_∞ . This value is independent of the inclination θ and the radius R of the trajectory.
2. For propeller airplanes: Use Ineqs. (42), which follows from the inequality $P_R \leq P_{Amax}$, to obtain the smallest possible angles of inclination θ_{min} , in terms of the speed V_∞ , with θ_{min} given by $\cos(\theta_{min})=s$. This inequality also yields an upper bound on the value for V_∞ , as the value at which s becomes null. For example, upon evaluating s at various V_∞ yields Table 1, for the Cessna 182. In this table, θ_{Hmax} is the angle of inclination with the horizontal plane, which we found more intuitively meaningful than θ .
3. For jet airplanes: Use the following inequalities that are required for $T_R \leq T_{Amax}$:
 - a. Ineqs. (50) and (52) to obtain an upper and a lower bound on the angle of inclination θ .
 - b. Ineq. (53) to obtain ranges of speeds V_∞ for a given θ .
4. Having thus determined what speeds Ineq. (42) allows for each angle of inclination, we complete the tables by entering in it all the minimum and maximum values of the average centripetal acceleration and of the radius that follow from the set of constraints we have derived.
5. Each table corresponds to a particular value of the angle of inclination θ . In the first line of the table, we write the value of θ , followed by the values of M_1 and m_1 , which are bounds on the average radial acceleration. They are put in the heading of the table because they are independent of the speed V_∞ . They are defined as follows:
 - c. M_1 =the upper bound on the average centripetal acceleration that corresponds to the upper bound on the load factor n , according to Ineq. (15).

Table 1 Values of the maximum angle of inclination with the horizontal θ_{Hmax} , in degrees, at various speeds, for the Cessna 182

V_∞	20	25	30	35	40	45	50	55	60	65	70	75
θ_{Hmax}	27.2	25.6	22.2	19.9	17.6	15.4	13.1	10.8	8.5	6.2	3.7	1.2

- d. m_1 =the lower bound on the average centripetal acceleration that is required by the non-negativity of the thrust, according to Ineq. (31).
- 6. The rest of the entries in these tables are the lower and upper bounds on the average centripetal acceleration, identified as follows.
 - e. M_2 =the upper bound that corresponds to the upper bound on C_L , according to Ineq. (17)
 - f. For propeller airplanes: M_3 =the upper bound that follows from $P_R \leq P_{Amax}$, according to Ineq. (46)
 - For jet airplanes: M_3 =the upper bound that follows from $T_R \leq T_{Amax}$, according to Ineq. (58)
 - g. $U=U(V_\infty, \theta)$ as defined in Eq. (25). According to Ineqs. (27) if $U \leq -1$ then the thrust required T_R is guaranteed to be non-negative. Otherwise, there will be the following lower bound on the average centripetal acceleration:
 - h. m_2 =the lower bound that corresponds to the RHS of Ineq. (35).
- 7. If the upper and lower bounds on the average centripetal acceleration are compatible, then the minimum and maximum values of the radius, as R_{min} and R_{max} are calculated and entered in the table. If some constraints are not respected then this indicates that this particular trajectory is not flyable by this airplane, and a “X” appears instead of the value of the radii.

10.1 Cessna 182

Ineq. (18) requires the following lower bound $V_\infty \geq 19.071$ m/s. Table 1 lists the possible angles of inclination for the various speeds. We shall compute the tables of possibilities for every speed V_∞ at every 5th value, from 20 to 65 m/s, and for the angle of inclination with the horizontal θ_H at each 5 degree from 5° to 15° . The entries for which $U \leq -1$ are highlighted in grey. Note that there are no speeds at which the Cessna 182 can fly a circular trajectory inclined by 15° or more with the horizontal at constant speed.

10.2 Silver Fox like UAV

Ineq. (18) requires the following lower bound $V_\infty \geq 11.067$ m/s. Fig. 11 shows the region in grey of the $(\cos(\theta), V_\infty)$ plane in which Ineq. (42), i.e., $\cos(\theta) \leq s$, is satisfied. Table 5 lists the corresponding possible angles of inclination for the various speeds.

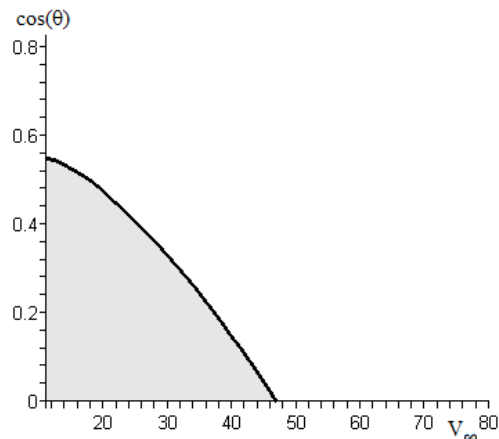
We shall compute the tables of possibilities for every speed V_∞ at every 5th value, from 15 to 40 m/s, and for the angle of inclination with the horizontal θ_H at each 5 degree from 5° to 30° . The

Table 2 Parameters that determine the flyability of trajectories inclined at $\theta_H=5^\circ$, for the Cessna 182

$\theta_H=5^\circ$	$M_1=3.58 \quad m_1=0.09$									
V_∞	20	25	30	35	40	45	50	55	60	65
M_2	0.38	1.31	2.18	3.13	4.20	5.39	6.71	8.170	9.76	11.49
M_3	1.84	2.21	2.51	2.74	2.90	2.97	2.93	2.74	2.33	1.45
U	-1.33	-1.01	-0.90	-0.91	-0.99	-1.11	-1.27	-1.47	-1.70	-1.95
m_2			0.43	0.49	0.23					
R_{min}	107.7	48.6	42.2	45.7	56.4	69.6	87.1	112.6	157.8	298.4
R_{max}	469.2	733.1	212.1	255.1	716.1	2375.1	2932.2	3548.0	4222.4	4955.4

Table 3 Parameters that determine the flyability of trajectories inclined at $\theta_H=10^\circ$, for the Cessna 182

	$\theta_H=10^\circ$			$M_1=3.50 \quad m_1=0.17$				
	20	25	30	35	40	45	50	55
V_∞	20	25	30	35	40	45	50	55
M_2	0.32	1.23	2.10	3.05	4.11	5.31	6.63	8.09
M_3	1.52	1.88	2.09	2.21	2.23	2.12	1.81	1.04
U	-0.65	-0.50	-0.45	-0.45	-0.49	-0.55	-0.64	-0.74
m_2	0.79	1.17	1.47	1.71	1.88	1.98	1.98	1.86
R_{\min}	X	51.7	44.0	56.5	73.1	97.4	X	X
R_{\max}	X	57.5	62.4	73.2	86.9	104.6	X	X

Fig. 11 Region in which $\cos(\theta) \leq s$, for the Silver Fox-like UAV, shown in grayTable 4 Values of the maximum angle of inclination with the horizontal $\theta_{H\max}$, in degrees, at various speeds, for the Silver Fox UAV

V_∞	15	20	25	30	35	40	45
$\theta_{H\max}$	31.760	28.217	23.933	19.164	14.000	8.427	2.459

Table 5 Parameters that determine the flyability of trajectories inclined at $\theta_H=5^\circ$, for the Silver Fox UAV

	$\theta_H=5^\circ$		$M_1=4.65 \quad m_1=0.09$			
	15	20	25	30	35	40
V_∞	15	20	25	30	35	40
M_2	1.46	3.02	4.92	7.19	9.86	12.94
M_3	3.42	4.31	4.91	5.13	4.80	3.40
U	-0.83	-0.98	-1.32	-1.78	-2.36	-3.04
m_2	0.63	0.30				
R_{\min}	17.8	13.50	13.0	17.9	26.0	48.0
R_{\max}	36.3	137.9	733.1	1055.6	1436.8	1876.6

entries for which $U \leq 1$ are highlighted in grey. Note that there are no speeds at which the Silver Fox can fly a circular trajectory inclined by 15° or more with the horizontal at constant speed.

Table 6 Parameters that determine the flyability of trajectories inclined at $\theta_H=10^\circ$, for the Silver Fox UAV

	$\theta_H=10^\circ$		$M_1=4.73 \quad m_1=0.17$		
V_∞	15	20	25	30	35
M_2	1.38	2.94	4.83	7.11	9.78
M_3	3.05	3.78	4.18	4.11	3.18
U	-0.41	-0.49	-0.66	-0.89	-1.19
m_2	1.68	2.09	2.13	1.43	
R_{\min}	X	13.9	15.2	22.4	39.3
R_{\max}	X	19.5	29.9	64.4	718.4

Table 7 Values of the maximum angle of inclination with the horizontal $\theta_{H\max}$, in degrees, at various speeds, for the F-16 jet fighter

θ_H	10	20	30	40	50	60	70	80	90
V_{\max}	509.8	475.0	439.9	405.6	373.6	345.4	323.2	308.9	303.9

Table 8 Parameters that determine the flyability of trajectories inclined at $\theta_H=10^\circ$, for the F-16 jet

	$\theta_H=10^\circ$		$M_1=8.77 \quad m_1=0.17$		
V_∞	100	200	300	400	500
M_2	3.09	13.41	30.46	54.30	84.95
M_3	4.43	8.52	11.29	11.56	4.55
U	-0.61	-1.22	-2.59	-4.55	-7.09
m_2	1.09				
R_{\min}	330.7	479.0	1046.9	1861.2	5602.9
R_{\max}	940.5	23457.7	52779.7	93830.6	1.47E5

Table 9 Parameters that determine the flyability of trajectories inclined at $\theta_H=30^\circ$, for the F-16 jet

	$\theta_H=30^\circ$		$M_1=8.46 \quad m_1=0.50$		
V_∞	100	200	300	400	
M_2	2.79	13.09	30.13	53.97	
M_3	3.72	7.09	8.79	6.69	
U	-0.19	-0.42	-0.90	-1.58	
m_2	2.71	4.50	2.85		
R_{\min}	365.3	576.1	1085.8	2441.2	
R_{\max}	376.7	907.4	3225.7	32653.1	

10.3 Lockheed Martin F-16

Ineq. (18), upper bound on C_L , requires the following lower bound $V_\infty \geq 54.192$ m/s. Ineqs. (50) and (52) are satisfied for all θ , since their RHS is larger than 1. For the F-16, the condition $V_\infty \leq V_\infty$ of Ineq. (53) is always satisfied. The condition $V_\infty \leq V_+$ yields the following table of possibilities.

We shall compute the tables of possibilities for every speed V_∞ at every 100 m/s, from 100 to

Table 10 Parameters that determine the flyability of trajectories inclined at $\theta_H=40^\circ$, for the F-16 jet

	$\theta_H=40^\circ$	$M_1=8.33 \quad m_1=0.64$		
V_∞	100	200	300	400
M_2	2.68	12.96	29.99	53.83
M_3	3.39	6.37	7.45	2.46
U	-0.13	-0.32	-0.70	-1.23
m_2	3.20	5.51	5.51	
R_{\min}	X	640.7	1232.1	6634.1
R_{\max}	X	740.2	1665.8	25391.2

500 m/s, and for the angle of inclination with the horizontal $\theta_H=10^\circ$, 30° and 40° . The entries for which $U \leq 1$ are highlighted in grey. Note that there are no speeds at which the F-16 can fly a circular trajectory inclined by 50° or more with the horizontal at constant speed.

11. Conclusions

We have obtained general formulas that correspond to necessary and sufficient conditions for airplanes to be able to travel inclined circular trajectories. We believe that they are original in that they have not been published before. They constitute an important tool for the analysis of airplane performances. Some of these conditions apply to any circular trajectory, whatever the speed profile at which it is flown, namely:

- Whatever its weight and propulsion system, all airplanes must bank by the same angle β in order to travel at a same speed V_∞ on a circular trajectory of radius R . This fact is well known for horizontal circular trajectories but, as we have proven, also hold for any trajectory inclined with respect to the horizontal plane.
- Both the lift L and $\cos(\beta)$ must keep the same sign at every point of the trajectory, and this sign has to be the same one for both of them.

For trajectories flown at constant speed:

- The bank angle is symmetrical through reflection in a vertical plane that goes through the lowest and highest points of the trajectory.
- The centripetal acceleration A_c remains positive and the bank angle keeps the same sign on the whole trajectory
- the load factor and the lift coefficient keep the same sign on the whole trajectory, which is that of the bank angle β and the lift L .
- the speed is bounded below according to Ineq. (18) that is independent of the radius and the angle of inclination of the trajectory
- some constraints on the speed and angle of inclination that are independent of the radius of the trajectory, and the thrust available
- a series of constraints on the average centripetal acceleration that ensures the thrust is non-negative and that it remains bounded above by the available thrust

These conditions can readily be used to test whether trajectories at a given speed and inclination are flyable. In Section 10, we have demonstrated a procedure that allows for the

production of tables of parameters for which trajectories are possible. We have done so for airplanes with a reciprocating engine and a constant speed propeller or with a fixed pitch propeller and airplanes with jet propulsion. The airplanes considered in the examples are similar to the Cessna 182 Skylane, the Silver Fox UAV and the F-16 Fighting Falcon. Such tables, as we have obtained, would be very useful when one does not want, or cannot, calculate on board the terms that appear in the inequalities that we have derived. When it comes to using them, it would be sufficient to store in them the angle θ_H , the speeds V_∞ together with the minimum and maximum radii for these parameters. Such tables could then readily be stored in a memory that even a small microcontroller could access. When considering a circular trajectory to be flown at a given angle, the tables could say if it is flyable, and if so, what the possible radii are for it. This approach would be completely appropriate for automatic trajectory planning.

References

- Aeronautics Learning Laboratory for Science Technology and Research (ALLSTAR) of the Florida International University (2011), Propeller Aircraft Performance and The Bootstrap Approach, available at the internet address <http://www.allstar.fiu.edu/aero/BA-Background.htm>
- Airliners.net web site (2015), at the internet address: <http://www.airliners.net/aircraft-data/stats.main?id=145>
- Ambrosino, G., Ariola, M., Ciniglio, U., Corraro, F., De Lellis, E. and Pironti, A. (2009), "Path generation and tracking in 3-D for UAVs", *IEEE Tran. Control Syst. Tech.*, **17**(4), 980-988.
- Anderson, J.D. Jr (2000), *Introduction to Flight*, Fourth Edition, McGraw-Hill Series in Aeronautical and Aerospace Engineering, Toronto, Ontario, Canada.
- Babaei, A.R. and Mortazavi, M. (2010), "Three-dimensional curvature-constrained trajectory planning based on in-flight waypoints", *J. Aircraft*, **47**(4), 1391-1398.
- Cavcar, M. (2004), *Propeller*, available at the website of the Anadolu University, School of Civil Aviation, Eskisehir, Turkey, at the address: <http://home.anadolu.edu.tr/~mcavcar/common/Propeller.pdf>
- Chandler, P., Rasmussen, S. and Pachter, M. (2000), "UAV cooperative path planning", *Proceedings of the AIAA Guidance, Navigation, and Control Conference*, Denver, Colorado, USA, August.
- Chitsaz, H. and LaValle, S.M. (2007), "Time-optimal Paths for a Dubins airplane", *46th IEEE Conference on Decision and Control*, New Orleans, Louisiana, USA, December.
- Cowley, W.L. and Levy, H. (1920), *Aeronautics Theory and Experiment*, 2nd Edition, Edward Arnold, London, England.
- Curawong Engineering (2015), UAV Engines, available at the internet address: http://www.curawongeng.com/products/uav_engines/
- Dubins, L.E. (1957), "On curves of minimal length with a constraint on average curvature and with prescribed initial and terminal positions and tangents", *Am. J. Math.*, **79**, 497-516.
- Faculty of Engineering, University of Porto (2013), SilverFox Block B-3 Specifications, available at the internet address: http://whale.fe.up.pt/asasf/images/f/f8/UAV_SF_Specs.pdf
- Filippone, A. (2000), "Data and performances of selected aircraft and rotorcraft", *Prog. Aerospace Sci.*, **36**, 629-654.
- Filippone, A. (2006), *Flight Performance of Fixed and Rotary Wing Aircraft*, American Institute of Aeronautics and Astronautics Education Series, Schetz, J.A. Series Editor-in-Chief, AIAA, Inc. and Butterworth-Heinemann, Herndon, Virginia, USA.
- Granelli, F. (2007), Carl Goldberg Falcon 56, The Academy of Model Aeronautics' Sport Aviator, the e-zine for the newer RC pilot, December, available at the internet address: <http://masportaviator.com/2007/12/01/carl-goldberg-falcon-56/>
- Horizon Hobby Inc. (2004), Introducing the new Hangar 9 Twist 40 ARF, information web site: <http://www.hangar-9.com/Articles/Article.aspx?ArticleID=1308>.

- Hota, S and Ghose, D. (2010), "Optimal geometrical path in 3D with curvature constraint", *IEEE/RSJ International Conference on Intelligent Robots and Systems (IROS)*, Taipei, Taiwan, October.
- Hwangbo, M., Kuffner, J. and Kanade, T. (2007), "Efficient two-phase 3D motion planning for small fixed-wing UAVs", *IEEE International Conference on Robotics and Automation*, Rome, Italy, April.
- Jia, D. and Vagners, J. (2004), "Parallel evolutionary algorithms for UAV path planning", *AIAA 1st Intelligent Systems Technical Conference*, Chicago, Illinois, September.
- Kingston, D.K. (2004), "Implementation issues of real-time trajectory generation on small UAVs", Master of Science Thesis, Department of Electrical and Computer Engineering, Brigham Young University, Provo, Utah, USA.
- Labonté, G. (2011), "Formulas for the fuel of climbing propeller driven planes", *Aircraft Eng. Aerosp. Tech.*, **84**(1), 23-36.
- Labonté, G. (2015), "Simple formulas for the fuel of climbing propeller driven airplanes", *Adv. Aircraft Spacecraft Sci.*, **2**(4), 367-389.
- Li, X., Xie, J., Cai, M., Xie, M. and Wang, Z. (2009), "Path planning for UAV based on improved A* algorithm", *9th International Conference on Electronic Measurement & Instruments, ICEMI '09*, 3-488-3-493, IEEE publishing, Beijing, China, August.
- Lockheed-Martin (2015), F-16 Specifications, available at the internet address: <http://lockheedmartin.com/us/products/f16/F-16Specifications.html>
- Mair, W.A. and Birdsall, D.L. (1992), *Aircraft Performance*, Cambridge Aerospace Series 5, Cambridge University Press, Cambridge, G.B.
- McIver, J. (2003), Cessna Skyhawk II /100, Performance Assessment, Temporal Images, Melbourne, Australia. Available at the internet address: <http://www.temporal.com.au/c172.pdf>
- Nikolos, I.K., Tsourveloudis, N.C. and Valavanis, K.P., (2003), "Evolutionary algorithm based 3-D path planner for UAV navigation", *IEEE Tran. Syst. Man Cyber. Part B: Cybernet.*, **33**(6), 898-912 .
- Phillips, W.F. (2004), *Mechanics of Flight*, John Wiley & Sons, Inc., Hoboken, New Jersey, USA
- Roud, O. and Bruckert D. (2006), Cessna 182 Training Manual, Published by Red Sky Ventures and Memel CATS, Second Edition 2011, Windhoek, Namibia.
- Sadraey, M. (2009), *Aircraft Performance Analysis*, VDM Verlag Dr. Müller, Saarbrücken, Germany.
- Stengel, R.F. (2004), *Flight Dynamics*, Princeton University Press, Princeton, New Jersey, USA.
- Von Mises, R. (1945), *Theory of Flight*, Dover Publications Inc., New York, New York, USA.
- Yang, K. and Sukkarieh, S. (2010), "An analytical continuous-curvature path-smoothing algorithm", *IEEE Tran. Robot.*, **26**(3), 561-568.
- Zheng, C., Ding, M. and Zhou, C. (2003), "Real-Time route planning for unmanned air vehicle with an evolutionary algorithm", *Int. J. Pattern Recog. Artif. Intel.*, **17**(1), 63-81.

Appendix A. Parameters of the representative airplanes

We have used for our example of calculations, the characteristics of the three representative airplanes that we list hereafter.

A.1 Cessna 182

Characteristic parameters for the Cessna 182 can be found in Airliners.net (2015), Roud and Bruckert (2006) and McIver (2003); those parameters that were not available were taken to have essentially the same values as those for the Cessna 172, which is similar to it.

Table A.1 Characteristic parameters of a Cessna 182 Skylane like airplane

$W_1 = 7,562.0$ N	$W_0 = 11,120.6$ N	$V_{\max} = 90$ m/s
$b = 11.02$ m	$S = 16.1653$ m ²	$e = 0.75$
$C_{L\max} = 2.10$	$C_{D0} = 0.029$	$n_{\max} = 3.8, n_{\min} = -1.52$
$P_{A\max} = 171.511$ kW, 2,600 rpm, at see level		
Propeller: constant speed, diameter = 2.08 m, $\eta_{\max} = 0.80$		

A.2 Silver Fox like UAV

The Silver Fox UAV is presently produced by Raytheon. Some of its specifications can be found at the Faculty of Engineering, University of Porto (2013). It has an off-the-shelf Radio Controlled engine that is described at Currawong Engineering (2015). Some of the parameters given below were estimated by comparison with similar small UAVs.

Table A.2 Characteristic parameters of a Silver Fox like UAV

$W_1 = 72.35$ N	$W_0 = 119.6$ N	$V_{\max} = 26$ m/s
$b = 2.4$ m	$S = 0.768$ m ²	$e = 0.8$
$C_{L\max} = 1.26$	$C_{D0} = 0.0251$	$n_{\max} = 5.0, n_{\min} = -2.0$
$P_{A\max} = 1,491$ W at 7,500 rpm, at see level		
Propeller: fixed pitch, diameter = 0.56 m, $\eta_{\max} = 0.83$		

A.3 Lockheed Martin F-16

The General Dynamics / Lockheed Martin F-16 Fighting Falcon is a single-engine fighter aircraft originally developed for the United States Air Force. Its characteristic parameters can be found in Lockheed-Martin (2015), Filippone (2000), Sadraey (2009). The maximum value of the lift coefficient and the maximum negative load factor were estimated from those of other similar fighter airplanes.

Table A.3 Characteristic parameters of an F-16 like airplane

$W_1 = 90,237.4$ N	$W_0 = 213,365.6$ N	$V_{\max} = 605$ m/s
$b = 10.0$ m	$S = 27.87$ m ²	$e = 0.8$
$C_{L\max} = 1.8$	$C_{D0} = 0.026$	$n_{\max} = 9.0, n_{\min} = -3$
$T_{A\max} = 131,222.5$ N		